

Comparison between RTM gradient and PSPI gradient in the process of FWI

Sergio Romahn, Marcelo Guarido and Kristopher Innanen

ABSTRACT

Full waveform inversion (FWI) can be described as an iterative cycle of four steps. Firstly, we generate synthetic seismic data (modelled shots) from a smoothed initial model and obtain the difference among observed and modelled shots (data residuals). Secondly, we migrate the data residual (using the current velocity model) and stack. This step produces the gradient. Thirdly, we scale the gradient in order to create a velocity update. And finally, we obtain a new velocity model by adding the velocity update to the current velocity model. We start another cycle by using the new velocity model. This report is focused in the second step of the cycle. Standard FWI uses reverse time migration (RTM) to obtain the gradient. On the other hand, iterative modelling, migration and inversion (IMMI) opens the door to use any type of migration method to produce the gradient. In this report, we compare the performance of the phase shift plus interpolation (PSPI) migration and RTM to obtain the gradient. We start pointing out the fundamental difference between these two methods: the fact that the first one is a one-way and the second one is a two-way wave operator. Then, we analyze the migration response and highlight the consequences of the previous point. Finally, we compare the inversion result by applying both methods. The PSPI and RTM gradients were scaled by applying the well calibration technique. We used synthetic data in an acoustic frame in this experiment. We found that both methods are suitable for producing the FWI gradient. However, the PSPI gradient is more sensitive to the initial velocity model than RTM, because its one-way wave operator does not recover long wavelengths as RTM does. This characteristic allows RTM producing a better inversion. PSPI would be a good option providing that the initial velocity model incorporates enough low frequency information. PSPI also showed a great sensitivity to the well interval coverage that is used to calibrate the gradient, while the RTM gradient is quite stable. We found that a hybrid inversion by using both methods is feasible and saves computational time.

INTRODUCTION

FWI and IMMI

FWI is a procedure that extracts information from seismic data by fitting observed and synthetic shots generated by wavefield modelling. Lailly (1983) was a pioneer in identifying the link between pre-stack migration and waveform seismic inversion. He described the inversion as a sequence of pre-stack migrations of the residuals and provided the mathematical basis for FWI. Contemporary to Lailly, Tarantola (1984) arrived at a similar idea: he explained the solution of the inverse problem as an iterative methodology that consists of a forward propagation of the actual sources in the current model and backward propagation of the data residuals. The correlation of the two fields yields to a correction of the model parameters. In other words, the full waveform inversion gradient is equivalent to a reverse time migration (RTM) of the data residuals. On the other hand, IMMI proposes the intu-

itive idea that any kind of depth migration will be able to produce the gradient (Margrave et al., 2010, 2012). Examples of experiments based on IMMI's approach, are the works of Pan et al. (2014), Margrave (2014), Guarido et al. (2014), Arenrin and Margrave (2015), and Romahn and Innanen (2017). The use of well-log data to scale the gradient is another example of IMMI. We will use this scaling technique in this work.

In this report, we analyze the performance of RTM and PSPI to produce the gradients. We start by highlighting fundamental differences of both methods through a comparison of their mathematical representations. Then we compare their gradient contribution by using a single interface model and a source-receiver pair. Finally, we use both type of gradients in the FWI process and compare the results. We also compare the sensitivity to the initial velocity model and to the well interval coverage in both methods.

RTM vs PSPI

RTM was introduced by Baysal et al. (1983), Whitmore (1983) and Chang and McMechan (1986). It uses a finite-difference solution to the wave equation and accounts for all arrival in the wavefield, including both primaries and multiples. Equation 1 is the 1D mathematical representation of RTM. A derivation of this equation and its equivalence to the FWI gradient can be found in Schuster (2017).

$$IM(z) = \int d\omega \omega^2 G(z, z_s, \omega) [G(z_g, z, \omega) D^*(\omega)] \quad (1)$$

where $IM(z)$ is the prestack RTM image at depth z , $G(z, z_s, \omega)$ is the forward propagation of source field to depth z , $G(z_g, z, \omega) D^*(\omega)$ is the backpropagation of the measured data D into the medium to the same depth, and the integral is the correlation of the two.

The FWI gradient g is shown in equation 2. The only difference between obtaining a prestack RTM seismic image and an RTM gradient is the data that we are migrating. For the first case, we migrate the measured seismic data, while for the second case we iteratively migrate the data residuals.

$$g^{(n)}(z) = \int d\omega \omega^2 G(z, z_s, \omega | s_o^{(n)}) [G(z_g, z, \omega | s_o^{(n)}) \delta P^*(z_g, z_s, \omega | s_o^{(n)})] \quad (2)$$

where g is gradient, n is iteration number, $G(z, z_s, \omega | s_o^{(n)})$ is the forward propagation of source field to depth z through the model parameter $s_o^{(n)}$, $G(z_g, z, \omega | s_o^{(n)}) \delta P^*(z_g, z_s, \omega | s_o^{(n)})$ is the backpropagation of the data residuals δP into the medium to the same depth.

Phase-shift migration was presented by Gazdag (1978). This frequency-wavenumber method is based on the exploding reflector model. It assumes that the sources are distributed along all reflectors, that the wavefield satisfies the scalar wave equation, and that the recorded seismic data are the values of the wavefield at the surface $u(x, z, t)$. We

can downward extrapolate (downward continuation) the data to simulate a seismic section that would be obtained if the recording plane was at depth z . Extrapolating the wavefield backwards in time to $t = 0$ when the sources were initiated, provides the migrated depth section $u(x, z, 0)$. The phase shift of the Fourier coefficients, in the frequency-wavenumber domain, produce the downward extrapolation of source and receiver positions. Equation 3 represents the migrated depth section under this methodology.

$$u(x, z, 0) = \frac{1}{4\pi^2} \int_{-\infty}^{\infty} \int_{-\infty}^{\infty} U(k_x, 0, \omega) \exp(ik_x x + ik_z z) dk_x d\omega \quad (3)$$

$$k_z = -\omega \sqrt{\frac{\omega^2}{V^2} - k_x^2} \quad (4)$$

where $U(k_x, 0, \omega)$ is the 2D Fourier transform of the wavefield $u(x, z, t)$, k_x are k_z are the radial horizontal and vertical wavenumbers, ω is the angular frequency, and V is velocity.

Phase shift migration fails in the presence of lateral velocity variations. In order to address this issue, Gazdag and Sguazzero (1984) conceived a generalization of this method that was called phase shift plus interpolation. The procedure is divided in two steps: 1) extrapolation of the wavefield by phase shift method using laterally uniform velocity fields l . The intermediate result is l reference wavefield. 2) Computation of the actual wavefield by interpolation of the reference wavefield.

We used the PSPI method modified by Ferguson and Margrave (2005). The algorithm accomplished prestack depth migration by the simultaneous downward continuation of shot records and model of the source wavefield. Multiples are not generated or handled because of the use of one-way wave operators. At each depth the two wavefields are compared in the space-frequency domain by using either the correlation imaging condition or the stabilized deconvolution imaging condition. The source simulation is done by seeding the 2D free-space Green's function into the computation at the first depth step.

Equations 1 and 3 show that RTM works with two-way wave operators (forward and backward propagation of source and receiver wavefields), while PSPI works with one-way wave operators. This fundamental difference allows RTM managing multiples, while PSPI only handles primaries. RTM is suitable for imaging complex geology such as salt bodies, while PSPI may have problems on this kind of geological settings. RTM may lead to much better resolution in the image providing an accurate velocity model, but it may be more sensitive to velocity errors. Computational cost and memory are important issues in RTM, while PSPI is relatively cheap.

MIGRATION RESPONSE

Figure 1 shows the two-layer model that was used to generate a single trace with a source-receiver pair separated by 1000 m. A minimum phase wavelet with a dominant frequency of 15 Hz was used as the seismic source. The migration of this trace by applying

RTM and PSPI is shown in figure 2. RTM computational time was 6 times longer than the time for PSPI migration. We use the cross-correlation imaging condition for this example. Three main events were identified in the migrated images. The source-and-receiver side reflection wavepaths B and C are formed by convolving the scattered wavefields caused by the reflector, and the forward and backward propagated wavefields are built by the source and the receiver. Event A is the migration ellipse. We cannot see the direct wave because its amplitude was overshadowed by the other events.

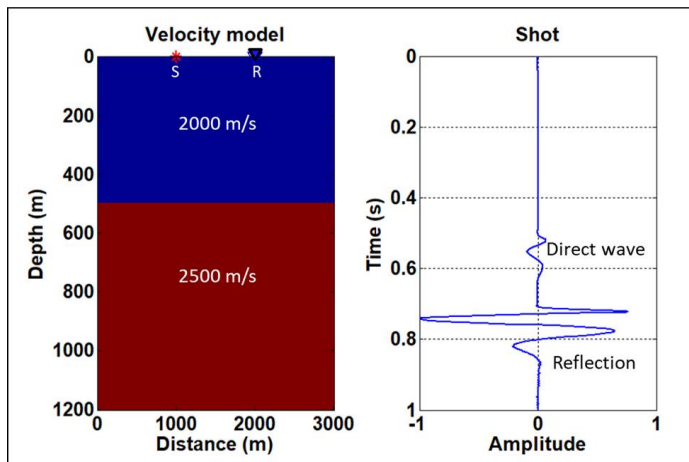


FIG. 1. Seismic trace generated by finite-difference modelling through a single interface model.

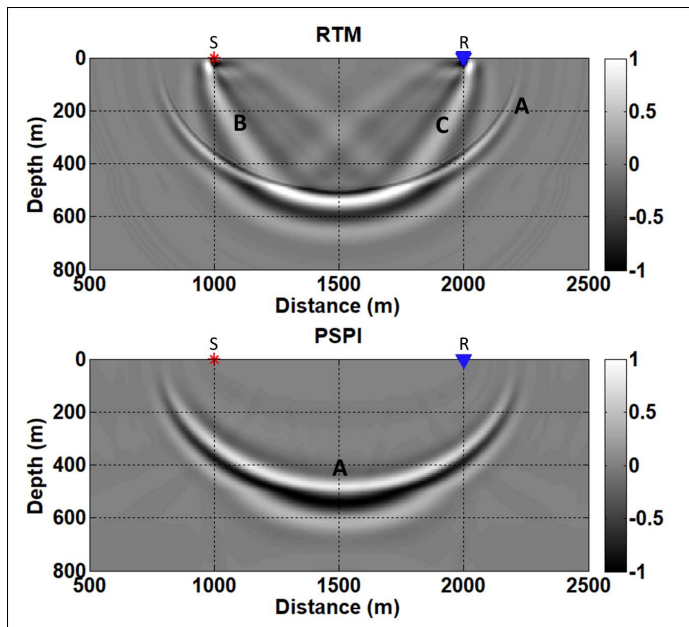


FIG. 2. PSPI and RTM applied to the 1000-m offset trace of figure 1 with cross-correlation imaging condition.

It has been shown that the deconvolution imaging condition works as a gain correction. For the case of the FWI gradient, it does something similar to the main diagonal elements of the inverse Hessian matrix (Margrave et al. (2010) and Pan et al. (2013)). We used

the model and the shot shown in figure 3 to compare cross-correlation to deconvolution imaging conditions for RTM and PSPI (figure 4). For the case of RTM, we observe that the gain provided by the deconvolution imaging condition is very subtle and probably not enough to completely correct the geometrical spreading. On the other hand, the gain that produces the deconvolution imaging condition, for the PSPI case, is very effective and is able to take the amplitude of the deeper reflection to the level of the shallow ones.

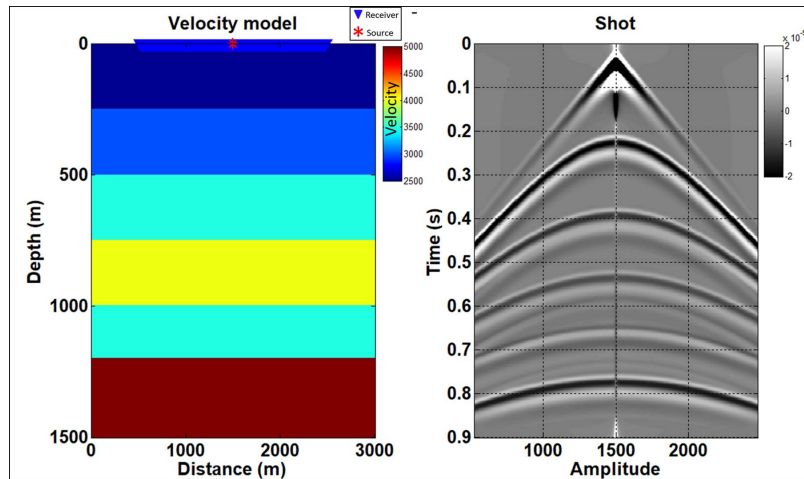


FIG. 3. Horizontal layered model used to generate the shot shown to the right hand side.

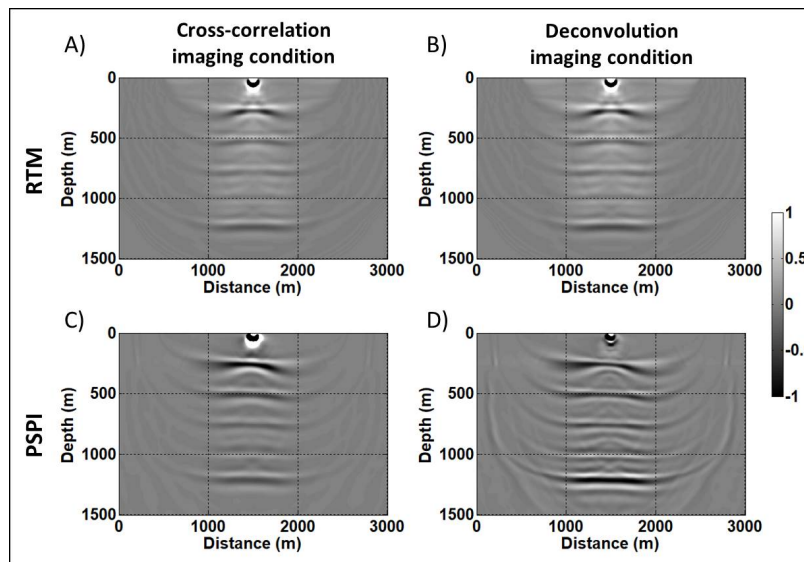


FIG. 4. Cross-correlation and deconvolution imaging conditions for RTM and PSPI applied to the shot of figure 3.

INVERSION METHODOLOGY

We inverted 81 synthetic seismic shots generated by solving the acoustic wave equation by finite differences with constant density. We used a minimum phase wavelet with dominant frequency of 20 Hz. The source and receiver intervals are 100 and 10 meters, respectively. The maximum offset is 2000 m. The velocity model to be solved corresponds

to a shallow syncline that constitutes a reservoir trap. The reservoir is characterized by a low P-wave velocity surrounded by a high velocity medium (figure 5). Examples of three seismic shots are shown in figure 6. The seismic survey contemplated fold taper and migration apron to define a zone where the performance of the inversion was evaluated. The error in the model was measured in the migration area with full fold and no border effects.

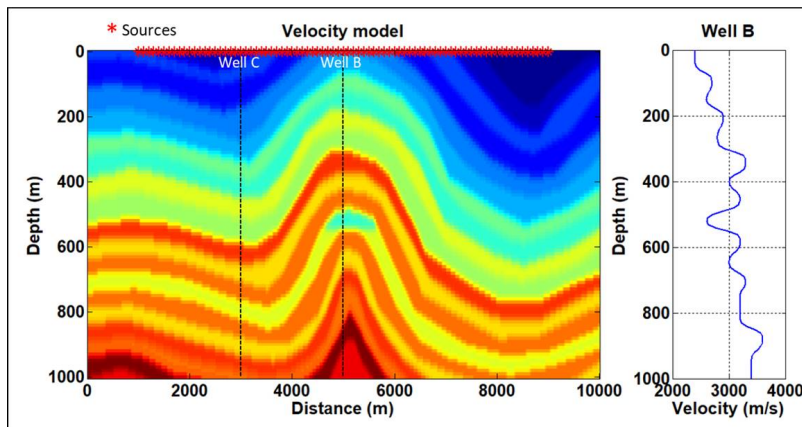


FIG. 5. Velocity model to be solved in the inversion.

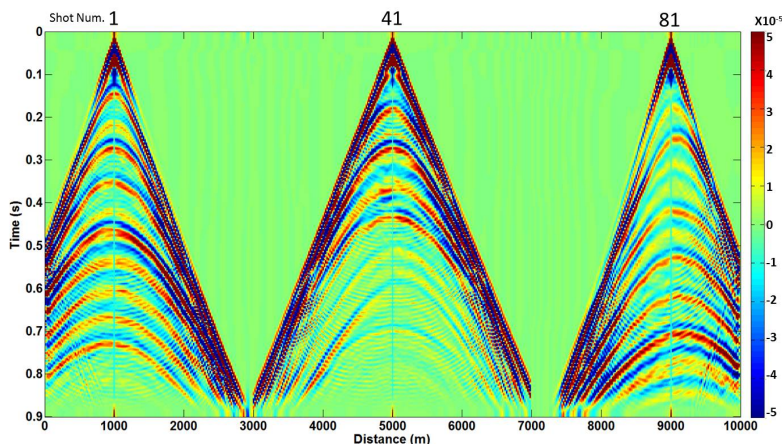


FIG. 6. Example of the synthetic seismic shots to be considered the observed data in the inversion.

FWI is an iterative process that can be seen as a cycle of four steps (Margrave et al., 2012).

1) The first step consists in the generation of synthetic seismic shots (modelled shots) from a smoothed initial model and calculation of the data residual (difference among observed and modelled shots).

The first iteration was done with an initial velocity model that was constructed by applying a Gaussian smoother to the true velocity model with a half-width of 300 m (figure 7-A). This model provides up to 3 Hz to start the inversion. Well C will be used to scale or calibrate the gradient, and well B will be used as a blind well to evaluate the inversion. The

modelled shots for this iteration are mainly constituted by the direct arrival (figure 7-B). There isn't any reflection because the smoothed initial model doesn't have a significant velocity contrast. The data residual will be the original shot with a slightly attenuated direct wave.

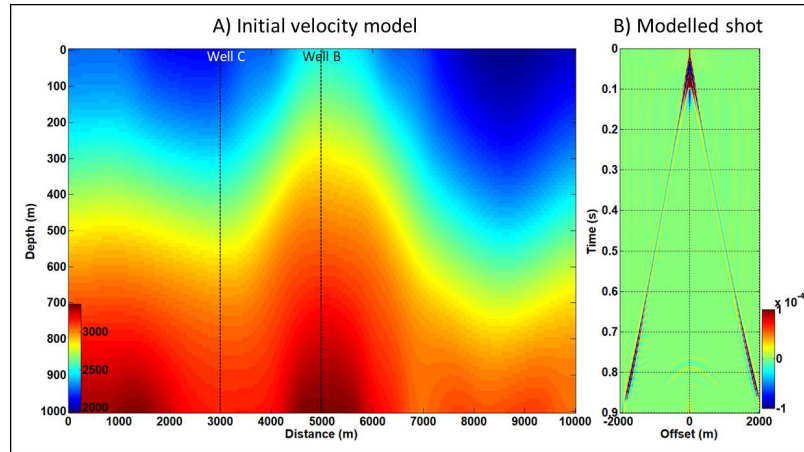


FIG. 7. A) Initial velocity model. B) Synthetic shot modelled by finite differences through the initial velocity model.

2) In the second step we apply pre-stack depth migration of the data residual (using the current velocity model) and stack.

We experimented with RTM and PSPI to migrate the data residuals in this stage of the cycle. We applied the multi-scale approach, where we start the inversion with low frequencies and introduce higher frequencies as we iterate. PSPI can naturally handle this technique because it allows selecting the frequency range that we want to migrate. For the RTM case, we have to filter the input data to migrate the desired frequencies. The frequency range for the first iteration was from 1 to 6 Hz. Then, we moved up the frequency band 1 Hertz in each of the following iterations. We used the deconvolution imaging condition for PSPI. This imaging condition works as a gain correction as illustrated by the example of the figure 3. We saw that the deconvolution imaging condition provided a weak gain for the case of RTM, so we opted to use the cross-correlation imaging condition with a standard gain correction computed as the radial distance from the shot to each image point. This is correct for a constant velocity medium; therefore, this conditioned RTM gradient is not the optimal. The result of stacking the migrated data residuals is the gradient. Figure 8-A and B show the gradient obtained with PSPI and RTM for the first iteration. The PSPI gradient has a strong event in the middle of the model, while the RTM gradient is better amplitude-balanced from the shallow to the deeper part. RTM provides more detail, specially of the anticline flanks.

3) The third step consists in scaling or calibrating the gradient by using well-log velocity. This step produces a velocity update.

The well calibration technique was described by Margrave et al. (2010). Firstly, the difference δvel between well and model velocities is calculated. The second step consists in estimating the amplitude scalar a and a phase rotation ϕ that make the gradient trace g more

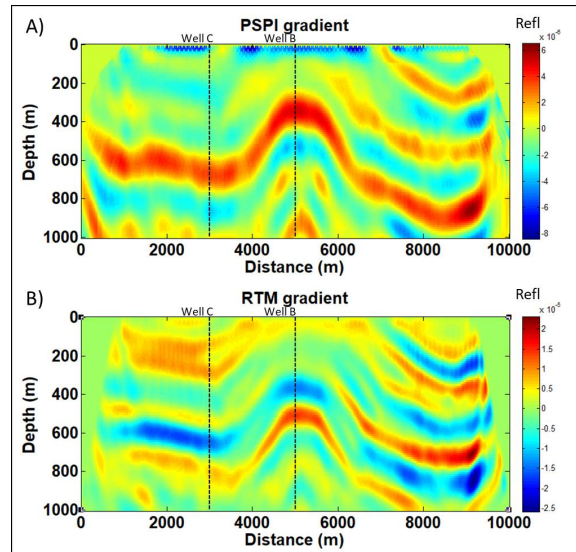


FIG. 8. A) PSPI gradient. B) RTM gradient.

like δvel . The scalar a is found such that $\delta vel - ag$ is minimized by least squares. Finally, a convolution matched filter is obtained with a and ϕ . This matched filter is applied to every gradient traces to obtain the velocity update. Figure 9-A and 9-B show the PSPI and RTM velocity updates for the first iteration. Well C provided the information to calibrate the gradient. For this example we used the whole well interval to do the calibration. Later we will show the sensitivity of both migration methods to the well interval.

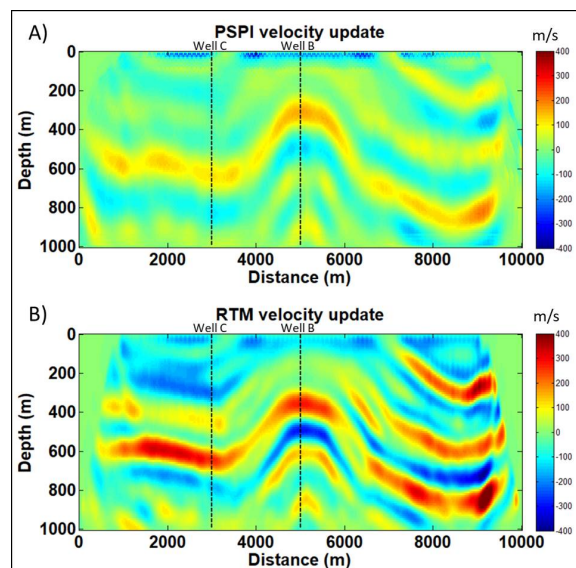


FIG. 9. A) PSPI velocity update. B) RTM velocity update.

4) The last step of the cycle corresponds to the sum of the current velocity model and the velocity update, providing a new model that will be used in the next iteration. The PSPI and RTM inverted velocity models for the first iteration are shown in figure 10. Although they

look very similar, the RTM inverted model is already defining some layers in the shallow part and provides a better definition of the geological target and the anticline flanks.

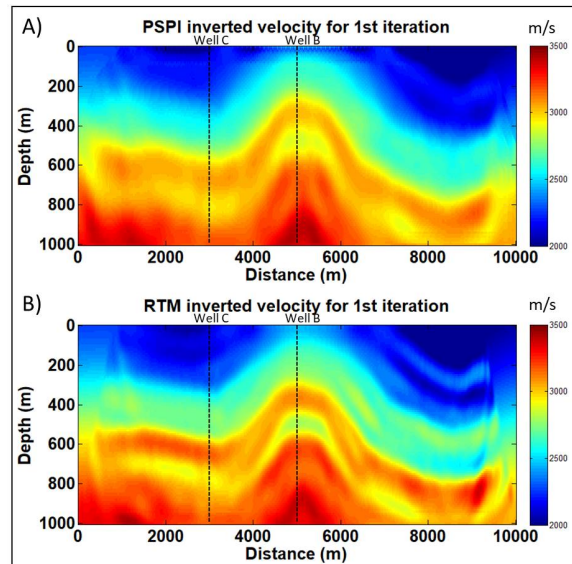


FIG. 10. Inverted velocity model for iteration 1 that result of summing up the velocity update and the initial velocity model. A) PSPI and B) RTM.

RESULTS

The final inverted velocity models obtained by using PSPI and RTM gradients after 15 iterations are shown in figure 11. A seismic survey can be divided by three zones: the full fold zone, the migration apron which is inside the full fold area, and the innermost zone beyond the migration apron which is the domain of the interpreter. All layers laying in this zone should be considered full-fold and fully migrated (Cordsen et al., 2000). The RTM model shows the best performance inside the interpreter zone. The error increases as we go to the borders of the survey and where the layers dip to that direction. RTM showed to be more sensitive to the seismic coverage than PSPI. The PSPI inverted model shows a large error in the area of the geological target, which suggests a poor performance of this migration method in the presence of high velocity contrasts.

The error in the model for PSPI and RTM is shown in figure 12. The error was calculated inside the full migrated zone with full fold and no border effects, between 3000 and 7000 m in the horizontal distance. RTM surpasses PSPI performance in the four first iterations, where we used frequencies between 1 and 9 Hz. The slope of the error curves is similar after the ninth iteration, which suggests that PSPI improves its efficiency in the high frequencies.

Sensitivity to the initial velocity model

The previous results were obtained by using an initial velocity model derived from smoothing the true velocity model with a half-width Gaussian smoother of 300 m. We increased the half-width to 600 m in order to test the sensitivity of both migration gradients to

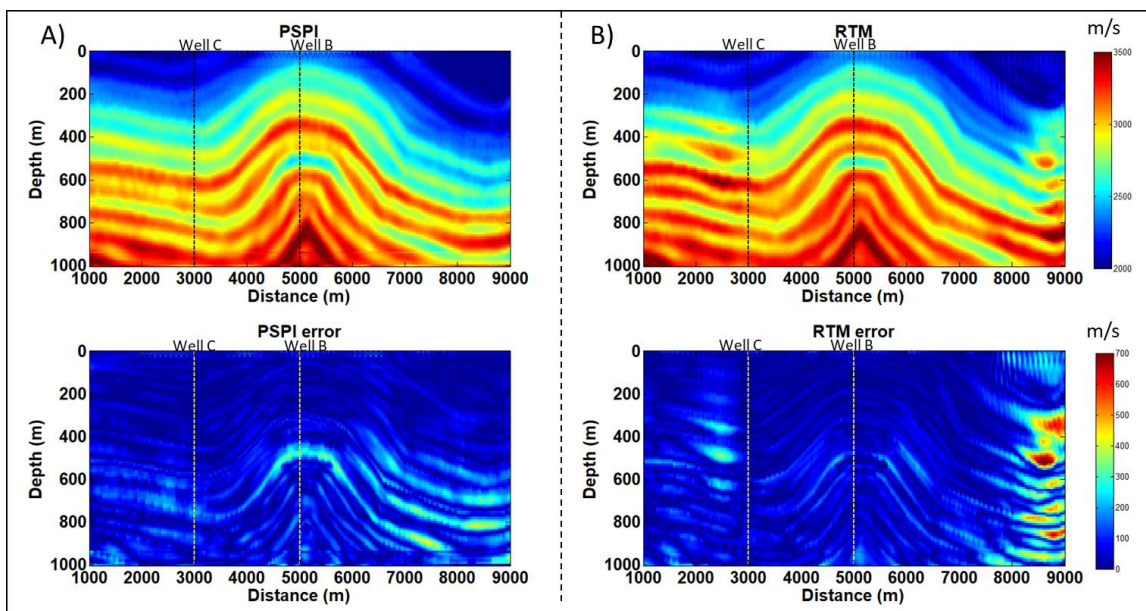


FIG. 11. Final inverted model after 15 iterations: A) PSPI and B) RTM.

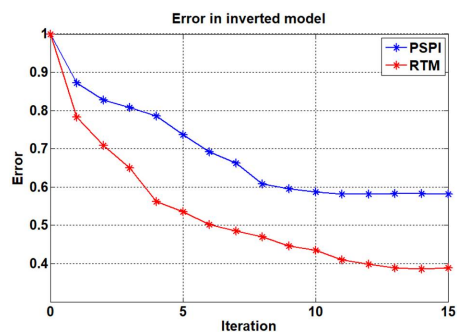


FIG. 12. Error in the inverted model for PSPI and RTM.

the initial velocity model. The comparison between the two initial models and the inverted velocities in the calibration well are shown in figure 13. PSPI inversion dramatically underperformed with a smoother initial model. RTM retrieves long wavelengths better than PSPI at a higher computational cost. The use of PSPI to obtain a satisfactory gradient will highly depend of how close the initial model is to the true model.

The results so far suggest that a hybrid inversion using both methods may help to achieve satisfactory results while allowing saving computational time. We propose the use of RTM for the firsts iterations, when we are introducing low frequencies, and then change to PSPI when we incorporate higher frequencies. The result of this approach is shown in figure 14. In the first two iterations we applied RTM and incorporated frequencies bellow 7 Hz. Iteration 3, 4, 5 and 6 were done by applying PSPI. The frequency bands for the PSPI iteration were: 1-15, 11-25, 21-35 and 31-45 Hertz. The inverted velocity model does not improves anymore after the 4th iterations. Other frequency strategies may produce different results. The hybrid inversion produces a superior result than PSPI alone with only 6

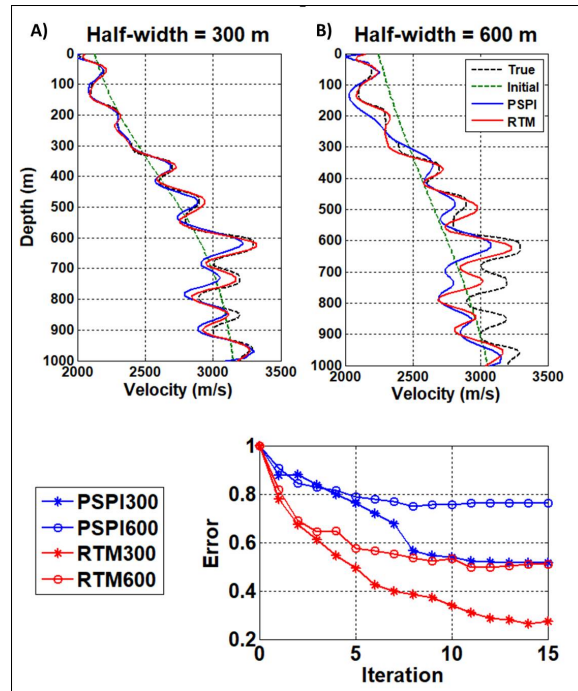


FIG. 13. Sensitivity to the initial velocity model of PSPI and RTM. A) Gaussian smoother half-width = 300 m. B) Gaussian smoother half-width = 600 m.

iterations. However, the result is not as good as the one obtained by using RTM alone in 15 iterations. The error with iteration for the three scenarios is shown in figure 15.

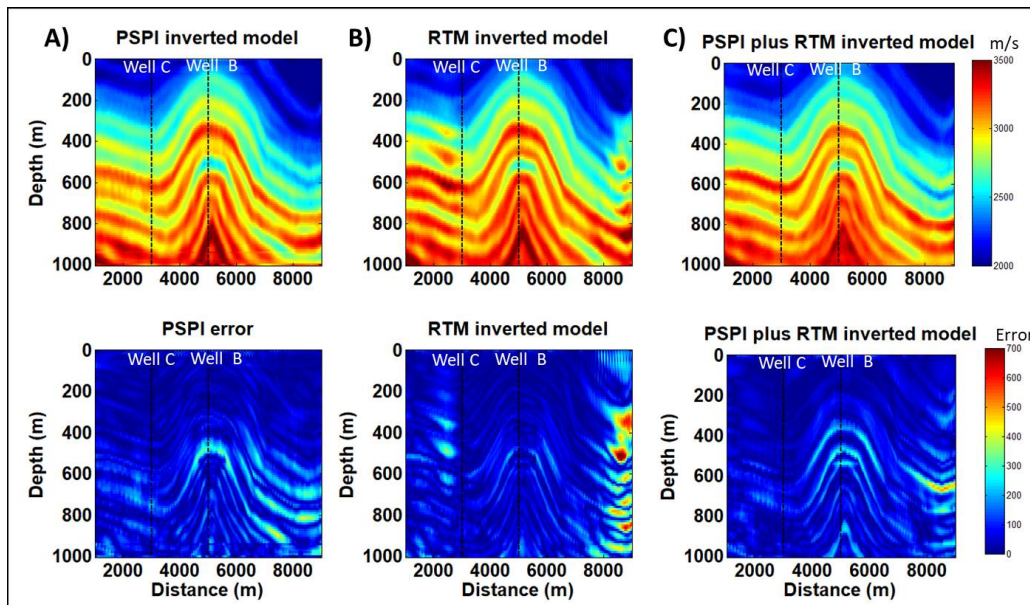


FIG. 14. A) PSPI final inversion. B) RTM final inversion. C) RTM plus PSPI final inversion

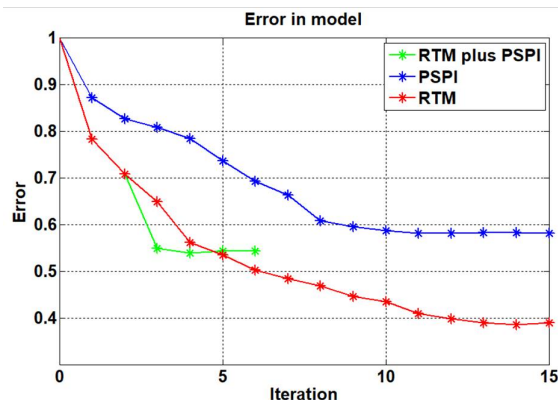


FIG. 15. Error in inverted model for PSPI, RTM and the combination of both of them.

Sensitivity to the well interval coverage

We used the whole well interval from zero to 1000 m in the previous examples. In this section, we tested the sensitivity of RTM and PSPI gradients with progressively smaller well interval coverages for the first iteration. Figure 16 shows the inverted velocity in the blind well and the error for different well intervals. We found that the RTM gradient produces a similar effect with different well coverages. On the other hand, PSPI gradient performance significantly degrades as the well coverage is reduced. As we mentioned before, the well calibration technique applies a convolution filter to the gradient in order to derive the update. This matched filter affects the gradient phase. This suggests that RTM gradient phase is very similar to the velocity update phase and does not rely on the calibration to correct the phase. On the other hand, the PSPI gradient may need to adapt its phase in order to be closer to the needed update, which will be strongly affected by the interval of calibration.

CONCLUSIONS

PSPI is a one-way wave migration method, while RTM uses two-way wave operators to perform the migration. This difference makes RTM more expensive, but also capable to manage all the arrivals in the wavefield, including primaries and multiples. The FWI gradient is commonly obtained by applying RTM to the data residuals. We showed that PSPI is also suitable to produce the gradient; however, it is more sensitive to the initial model and the well interval coverage used for the calibration, this characteristic will limit its applicability. RTM has the capability of recovering long-wavelength information; therefore, it is less sensitive than PSPI to a smoother initial model. The calibration of the RTM gradient with well information showed to be quite stable with smaller well interval coverages. In our synthetic example, RTM produced the smaller errors across the model and a superior result inside the full-fold and fully migrated zone. RTM showed to be more sensitive to the seismic coverage than PSPI. The better result provided by RTM comes with a higher computational cost. A migration of one shot with RTM took 6 times longer than PSPI. A hybrid inversion by using both methods is feasible and will save computational time, providing that we have enough well coverage to calibrate the PSPI gradient. RTM can be used in the first iterations when we use low frequencies to recover long wavelengths, and then

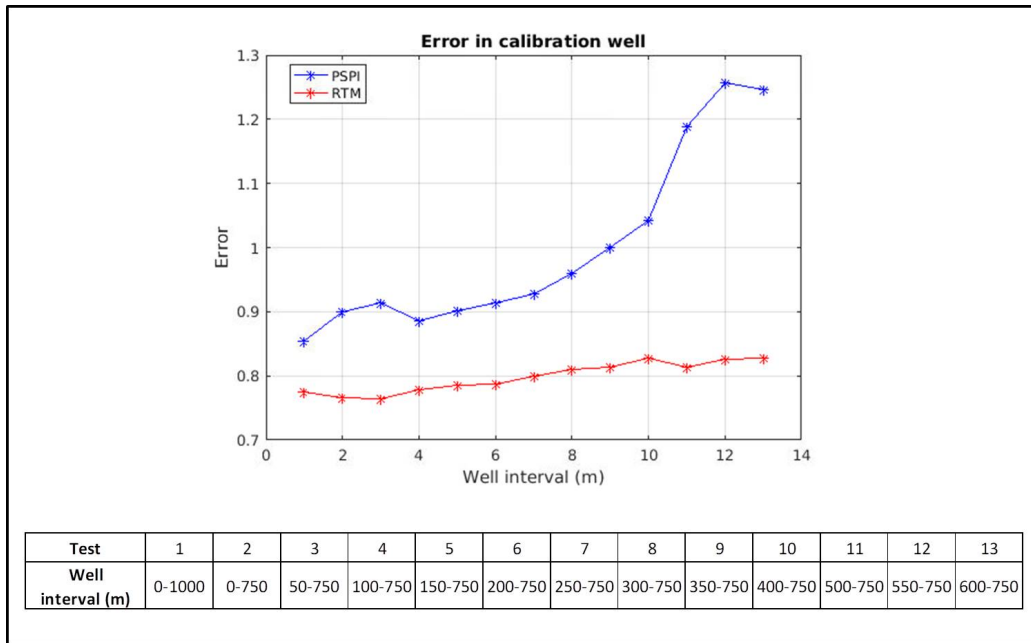


FIG. 16. Sensitivity of PSPI and RTM with well interval coverage for the first iteration (1-6 Hz).

PSPI can be used when we incorporate high frequencies to add detail to the model.

ACKNOWLEDGEMENTS

We thank the sponsors of CREWES for their support. We also acknowledge support from NSERC through the grant CRDPJ 461179-13. Author 1 thanks PEMEX and the government of Mexico for founding his research.

REFERENCES

Arenrin, B., and Margrave, G. F., 2015, Full waveform inversion of hussar synthetics: CREWES Research Report, **27**.

Baysal, E., Kosloff, D. D., and Sherwood, J. W. C., 1983, Reverse time migration: *Geophysics*, **48**, No. 11, 1514–1524.

Chang, W.-F., and McMechan, G. A., 1986, Reverse-time migration of offset vertical seismic profiling data using the excitation-time imaging condition: *Geophysics*, **51**, No. 1, 67–84.

Cordson, A., Galbraith, M., and Peirce, J., 2000, Planning land 3-D seismic surveys: Society of Exploration Geophysicists.

Ferguson, R. J., and Margrave, G. F., 2005, Planned seismic imaging using explicit one-way operators: *Geophysics*, **70**, No. 5, S101–S109.

Gazdag, J., 1978, Wave equation migration with the phase-shift method: *Geophysics*, **43**, No. 7, 1342–1351.

Gazdag, J., and Sguazzero, P., 1984, Migration of seismic data by phase shift plus interpolation: *Geophysics*, **49**, No. 2, 124–131.

Guarido, M., Lines, L., and Ferguson, R., 2014, Full waveform inversion - a synthetic test using the pspi migration: CREWES Research Report, **26**.

- Lailly, P., 1983, The seismic inverse problem as a sequence of before stack migration: SIAM, 206–220.
- Margrave, G. F., 2014, Post-stack iterative modeling migration and inversion (immi): CREWES Research Report, **27**.
- Margrave, G. F., Ferguson, R. J., and Hogan, C. M., 2010, Full-waveform inversion with wave equation migration and well control: CREWES Research Report, **22**.
- Margrave, G. F., Innanen, K. A., and Yedlin, M., 2012, A perspective on full-waveform inversion: CREWES Research Report, **24**.
- Pan, W., Innanen, K. A., and Margrave, G. F., 2013, Efficient pseudo gauss-newton full waveform inversion in the time-ray parameter domain: CREWES Research Report, **25**.
- Pan, W., Margrave, G. F., and Innanen, K. A., 2014, Iterative modeling migration and inversion (immi): Combining full waveform inversion with standard inversion methodology: 84th Ann. Internat. Mtg., SEG, Expanded Abstracts, 938–943.
- Romahn, S., and Innanen, K. A., 2017, Iterative modeling, migration, and inversion: Evaluating the well-calibration technique to scale the gradient in the full waveform inversion process: SEG Technical Program Expanded Abstracts 2017, 1583–1587.
- Schuster, G. T., 2017, Seismic inversion.
- Tarantola, A., 1984, Inversion of seismic reflection data in the acoustic approximation: Geophysics, **49**, 1259–1266.
- Whitmore, N., 1983, Iterative depth migration by backward time propagation, *in* SEG Technical Program Expanded Abstracts 1983, Society of Exploration Geophysicists, 382–385.